

The effects of deforestation and climate variability on the streamflow of the Araguaia River, Brazil

M. T. Coe · E. M. Latrubesse · M. E. Ferreira ·
M. L. Amsler

Received: 1 March 2010 / Accepted: 3 February 2011
© Springer Science+Business Media B.V. 2011

Abstract Deforestation changes the hydrological, geomorphological, and biochemical states of streams by decreasing evapotranspiration on the land surface and increasing runoff, river discharge, erosion and sediment fluxes from the land surface. Deforestation has removed about 55% of the native vegetation and significantly altered the hydrological and morphological characteristics of an 82,632 km² watershed of the Araguaia River in east-central Brazil. Observed discharge increased by 25% from the 1970s to the 1990s and computer simulations suggest that about 2/3 of the increase is from deforestation, the remaining 1/3 from climate variability. Changes of this scale

are likely occurring throughout the 2,000,000 km² savannah region of central Brazil.

Keywords Cerrado · Discharge · Deforestation · Land cover change · Araguaia River · Geomorphology

Introduction

Tropical South America encompasses the world's largest continuous tropical forest and savannah ecosystem, and generates about 25% of the global river discharge (Latrubesse 2008). In Brazil regional development pressures and increased global demand for cattle feed (e.g. soy), beef, and other agricultural commodities (e.g. sugar cane) have driven high rates of deforestation, over the last 4 decades (Achard et al. 2002; Fearnside 2005; Kaimowitz et al. 2004).

Although deforestation of the Amazon rainforest has been the primary focus of environmentalists and the press during recent decades, most of the tropical deforestation has taken place, and continues to take place in the savannah environments of central Brazil (locally known as Cerrado, Fig. 1) (Klink and Machado 2005). Of the original 2,000,000 km² of Cerrado that existed in Brazil more than 50% has been converted and fragmented by deforestation and expansion of the agriculture frontier (Sano et al.

M. T. Coe (✉)
The Woods Hole Research Center, 149 Woods Hole Rd,
Falmouth, MA 02540, USA
e-mail: mtcoe@whrc.org

E. M. Latrubesse
Department of Geography and the Environment,
University of Texas at Austin, A3100 GRG, Austin,
TX 78712, USA

M. E. Ferreira
Instituto de Estudos Sócio-Ambientais (IESA),
Universidade Federal de Goiás, 74001-970 Goiânia,
GO, Brazil

M. L. Amsler
Instituto Nacional de Limnología (INALI), Universidad
Nacional del Litoral-CONICET-CC217, 3000 Santa Fe,
Argentina

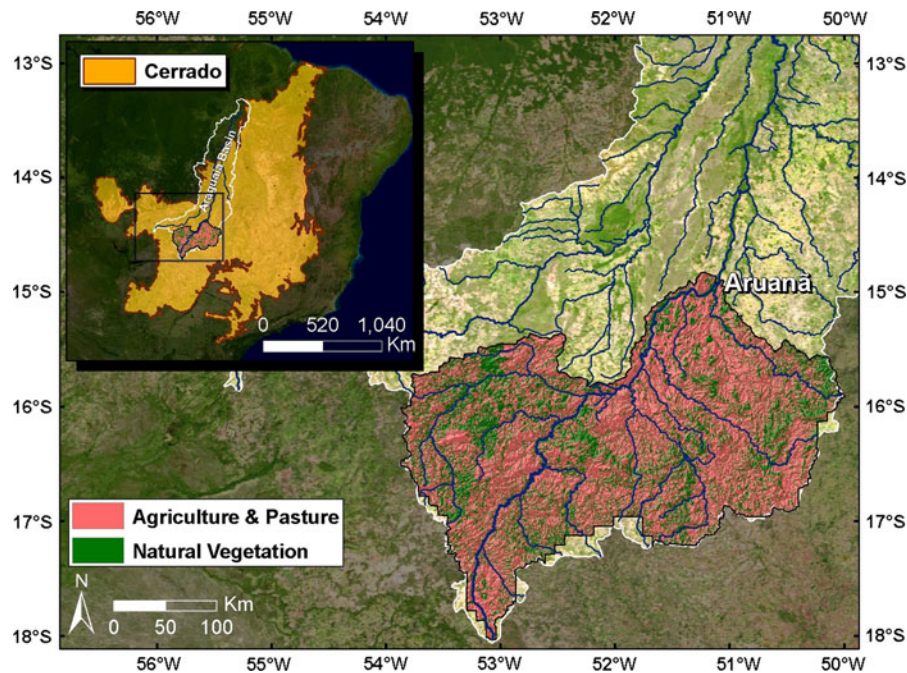


Fig. 1 Main figure: The 82,632 km² Araguaia River watershed upstream of Aruanã showing classification of remnant Cerrado and altered lands. About 54% of the basin vegetation was altered as of 2002. Inset: Eastern South

America showing the 2,000,000 km² Cerrado region. The Araguaia River basin is outlined and the region of study, the Aruanã watershed is shaded as in the main figure

2008). The Cerrado is considered a hot spot for biodiversity (Myers et al. 2000) and is the headwater region of the major rivers of eastern South America, but the policies of conservation and the attentions of society, science, and media have been insignificant in comparison.

Deforestation changes the hydrological, geomorphological, and biochemical states of streams (Bonan et al. 2004). Anthropogenic changes in vegetation generally result in increased discharge because annual crops and perennial pastures have reduced root density and depth, plant leaf area index (LAI), and growing season length, hence, lower evapotranspiration compared to the more diverse natural vegetation systems that they have replaced (Canadell et al. 1996; Costa et al. 2003; Eagleson 1978; Gardner 1983; Li et al. 2007; Raymond et al. 2008). Deforestation also often results in increased erosion from the land surface and deposition in channels and on floodplains because of the increased area of bare soil, changes in infiltration and surface runoff, and poor management practices (Bruijnzeel 1990; Dunne and Leopold 1978; Knox 1972).

Costa et al. (2003) analyzed discharge and climate data in a 175,000 km² sub-basin of the Tocantins watershed in eastern Amazônia and concluded that most of the observed 25% increase in discharge in that watershed was attributable to deforestation. Coe et al. (2009) used ecosystem models on that same watershed to show that climate variability alone could not explain the observed increased discharge in the Tocantins. Their results suggest that about 2/3 of the observed 25% increase in discharge in the last 50 years was a function of deforestation that occurred during that period.

Latrubesse et al. (2009) showed that large changes in sediment load and river morphology have occurred throughout a 120,000 km² basin of the Araguaia River coincident with the large land cover changes. Fieldwork and imagery analyses indicated a significant increase in sandy bed-load sediment transport, 232 million tons of stored sediment in the main channel, an increase in the number of sandy bars, and a 30% decrease in the number of small islands, most of which has occurred since the mid-1970s. Their results indicated that the river is in the process of

fundamentally altering its morphology to fill side channels and open a central corridor to more effectively transport the increased sediment flux. They concluded that the Araguaia is a rare example of rapid geomorphologic response of a large alluvial river to land cover and land use change.

Here we present an analysis of discharge data, climate data, and numerical model output of an about 82,600 km² basin of the Araguaia River. This watershed is part of the watershed studied by Latrubesse et al. (2009) and is adjacent to the Tocantins River studied by Costa et al. (2003) and Coe et al. (2009). In this study we quantify how deforestation, which began in the late 1960s, has significantly altered the hydrological characteristics of the otherwise unmodified Araguaia River.

Methodology

Region of study

The Araguaia River (Fig. 1) is a 385,000 km² watershed in eastern Amazonia with mean annual discharge of about 6,500 m³/s (comparable to the Danube). The 82,632 km² Araguaia sub-watershed upstream of the Aruanã stream gauge, where our study is based (Fig. 1), is in the center of agricultural production, particularly cattle, for the state of Goiás. Average annual precipitation for the period 1971–2000 is about 1730 mm/yr, 90% of which occurs in a 7-month period from October to April. Cerrado vegetation, which is composed of mixed grass and dry-season deciduous low-stature trees and shrubs, accounted for almost all of the watershed area before deforestation. Tree cover in this Cerrado environment can be as much as 70% and as little as 10–20%, depending on the local environment. Tall-stature gallery forests have historically been present only in isolated lowland areas on floodplains.

Large-scale land cover change in this watershed began in the late 1960s with conversion of Cerrado to native pasture by removing most or all of the native trees and shrubs to maximize grassland area. Land use increased and intensified in the 1970s, 80s, and 90s. Native pasture continued to replace Cerrado, while older native pasture was in turn progressively replaced by cultivated pasture, by felling trees, burning, and cultivation of non-native high yield

grass species (predominantly *Brachiaria*). Mechanized agriculture, predominantly soy, was also introduced on a smaller scale. By 2002, this conversion resulted in about 40% of the Aruanã watershed being in native and cultivated pasture, 15% in agriculture, and 45% in Cerrado and remnant forest (Sano et al. 2008, 2009).

In general, trees and shrubs in the Cerrado have greater above-ground woody plant density and biomass, deeper root systems, higher LAI, and support greater photosynthetic activity than the native and cultivated grass species, particularly in the long dry season (Garcia-Montiel et al. 2008; Meinzer et al. 1999b; Oliveira et al. 2005; Scholz et al. 2008). Deeper-rooted tree species may also redistribute water from deeper, wetter soil layers to shallower dryer layers during the dry season (Meinzer et al. 2004; Moreira et al. 2003; Scholz et al. 2002, 2008). Despite the fact that there can be important differences in the energy and water balances within any vegetation type (Ferreira et al. in prep; Santos et al. 2004), a general pattern of increased evapotranspiration, decreased sensible heat flux and decreased surface temperature occurs across a gradient from low (grasses) to high (dense tall trees) above-ground biomass (Ferreira et al. in prep; Giambelluca et al. 2009; Meinzer et al. 1999a, b; Santos et al. 2004). Therefore, anthropogenic changes in vegetation can potentially have significant impacts on the energy and water balance of the Cerrado region. The Araguaia watershed upstream of Aruanã is an excellent location to test for a direct influence of land cover change because continuous discharge measurements have been recorded since 1970 at the Aruanã gauge station (Fig. 1). These measurements began before deforestation was extensive, and no major direct alterations of the channel such as dam or levee construction have occurred.

Discharge and climate data analysis

To understand the impact of land cover change on the observed discharge and climate of the Araguaia we chose a data analysis approach based on that of Costa et al. (Costa et al. 2003). Two decadal means of discharge from the same gauge, separated from one another by one decade were examined.

We compare the discharge and precipitation of the 1970s (1970–1979) with that of the 1990s

(1990–1999). Sufficient data was not available to examine the period after the 1990s. The 1970s corresponded to the time of low land cover change, the 1990s high land cover change. The 1980s (1980–1989) decade was not used in this study in order to maximize the land cover difference between the decades being compared and the probability of detecting change in the discharge and climate.

Discharge measurements were taken from the Aruanã gauge station (Fig. 1, 51° 4' 56.75''W, 14° 55' 17.29''S, made available by the Agência Nacional de Águas <http://www.ana.gov.br>). Monthly mean values were created from the daily reported values. March, April and May of 1970 were missing therefore there are 117 months in the 1970s series and 120 months in the 1990s series. A classical *z*-test was used for comparison of the differences of the 237 months of discharge in the 1970s and 1990s time series. A *z*-test was appropriate in cases such as this, where the sample size is relatively large. From these monthly series decadal mean values for each month (i.e. 12 values January–December for each decade) and one annual mean value for each decade were also created. A Student's *t*-test, which was appropriate for small sample size, was used for comparison of the differences of the 12 monthly means of discharge and precipitation in the 1970s and 1990s time series.

Monthly mean precipitation data from the CRU-ts2.0 dataset (Mitchell et al. 2004) were used in this study for comparison with the observed and simulated discharge data. The CRU-ts2.0 is a $\frac{1}{2}^\circ \times \frac{1}{2}^\circ$ globally gridded monthly climate dataset for the period 1901–2000. It was derived by spatial interpolation of meteorological station data (Mitchell et al. 2004). The monthly $\frac{1}{2}^\circ$ values were spatially averaged over the 82,632 km² Aruanã watershed to create one mean value for each month for the entire basin. As with the discharge data, decadal values for each month and annual mean values were created for the 1970s and 1990s.

There is considerable variation among gridded precipitation datasets for the Amazon basin (Costa and Foley 1997). Techniques for precipitation measurement at a given location are well known and associated errors in the monthly means are low, generally 5% or less (Fetter 2001). However, derivation of a spatially extensive precipitation dataset requires interpolation in space between relatively sparsely distributed gauges or augmentation of data from other sources such as

satellite products or numerical model output, all of which can introduce significant error. Therefore, the quality of the CRU-ts2.0 dataset is assessed against observed discharge and other precipitation datasets to assure that it would be adequate for this project. Discharge data are a good source for comparison because measurement errors are also low and a measurement at one location explicitly integrates results from the entire area of the watershed.

Two other commonly used precipitation datasets, the CPC Merged Analysis of Precipitation, (CMAP, Xie and Arkin 1997), and NCEP/NCAR Reanalysis (NCEP, Kalnay et al. 1996; Kistler 2001), are compared to help further assess the quality of the CRU-ts2.0 precipitation data. The CRU-ts2.0 data is based only on rain gauge data; CMAP is a 2.5° horizontal resolution merged satellite and rain gauge dataset, while NCEP is a 2.5° horizontal resolution model reanalysis product. For each dataset a spatially averaged value of monthly and annual mean precipitation are created for the Aruanã watershed for the period 1979–1998. This particular time period is the longest period for which all datasets overlapped.

For the 20-year period the mean annual precipitation rate of the CRU-ts2.0 dataset is 1748 mm/yr (Table 1). This value is between the estimates of the

Table 1 Comparison of precipitation data sets

	lag	CRU-ts2.0	CMAP	NCEP
Annual mean (mm/yr)		1748	1464	1916
Monthly correlation	0	0.61588	0.65044	0.55004
	−1	0.83509	0.81004	0.67728
	−2	0.74812	0.69013	0.64314
Annual correlation	−1	0.61337	0.16297	−0.17889

Monthly mean precipitation summed over the Aruanã watershed in mm/yr from the CRU05, CMAP, and NCEP data products. Monthly correlation is the Pearson product moment coefficient of correlation (*r*) of the 240 monthly mean values of precipitation to the observed discharge for the period 1979–1998. Annual correlation is the coefficient of correlation (*r*) of the 19 annual mean water-years for the period 1980–1998. Numbers in the second column of the correlation rows represent the number of months of lag between the precipitation and discharge correlation. Therefore, a lag of −1 means discharge in January is correlated to precipitation of December. For the annual correlation the 1-month lag is represented in the calculation of the water year; the water year is defined as September to August for the precipitation and October to September for the discharge and is named for the year in which the average ends

other two products (Table 1). The CMAP precipitation rate is 1464 mm/yr, 16% less than the CRU-ts2.0 and the NCEP precipitation rate is 1916 mm/yr, about 10% greater than the CRU-ts2.0.

The Pearson product moment coefficient of correlation (r) was applied to the 240 months of each data set to measure the linear agreement of the mean seasonal cycle of the precipitation and discharge. 0, 1, and 2-month time lags were applied to the comparison. For example, the discharge of February 1980 was compared to the precipitation of January 1980 when a 1-month lag is applied and December 1979 when a 2-month lag is applied. In all cases the coefficient of correlation was greatest when a 1-month time lag was used (Table 1, Fig. 2), which indicates that on average there is a 1-month lag in the response time of the hydrologic system at the gauge to the upstream precipitation input. CRU-ts2.0 had the highest level of agreement of the monthly precipitation to the discharge ($r = 0.83509$), followed by CMAP (0.81004), and the NCEP reanalysis product (0.67728), suggesting that CRU-ts2.0 among the three best represented the seasonal hydrologic cycle.

Annual mean precipitation and discharge were calculated for each water-year in the 20-year series. The water-year was defined as beginning in September and ending in August for the precipitation data (e.g. water-year 1980 is the mean of September 1979 to August 1980) and October to September for the

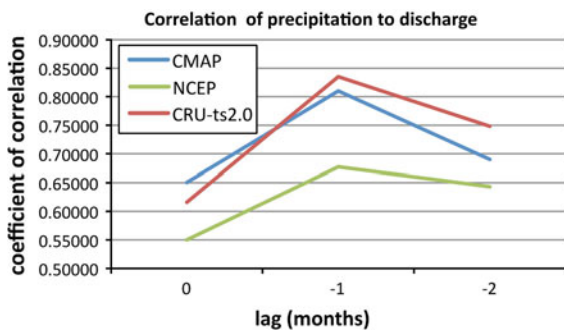


Fig. 2 Lagged Pearson product moment coefficient of correlation (r) between the 228 monthly mean precipitation and discharge values for the period 1980–1998. Values are spatially averaged over the 82,632 km² Aruanã watershed for the CRU-ts2.0, NCEP, and CMAP datasets. All data show best linear relationship of precipitation to discharge when the month of peak precipitation lags the discharge peak by 1-month (−1)

discharge. Nineteen full water years (1980–1998) were created from the 20 years of data. 1978 data were not available in the CMAP dataset to create a 1979 mean water-year, therefore to maintain consistency it was not calculated for any of them. The Pearson coefficient of correlation was used to measure the agreement of the inter-annual variability of the 19 years of the observed mean precipitation and discharge data. CRU05 had the highest coefficient of correlation ($r = 0.61337$). The coefficient of correlation between the CMAP and NCEP mean annual precipitation and the observed discharge was 0.16297 and -0.17889 , respectively (Table 1, Fig. 3), which suggested little correlation of the interannual variability of these precipitation data sets to the observed discharge. The analysis suggested that of the available datasets CRU05 best represented the climate of the region and was appropriate for use in the IBIS land surface model.

Numerical modeling of discharge

A series of simulations over the Araguaia basin were made with the IBIS/THMB ecosystem models to evaluate the potential scale of the individual contributions of land cover change and climate variation to the observed discharge change.

Numerical models

IBIS is a physically-based dynamic vegetation and land surface model that simulates the energy, water, and carbon balance of the soil–vegetation–atmosphere system as a linked set of equations (Kucharik et al. 2000). Structurally, the model has two vegetation canopies, an upper canopy of trees and a lower canopy of grasses, shrubs, and crops with a total of 12 plant functional types. The model is driven by input data of above-canopy temperature, humidity, wind speed, precipitation, and incoming short and long-wave radiation. IBIS calculates the temperature of the soil surface and canopy and the temperature and humidity of the air within the canopy as a function of the radiative balance of the vegetation and land surface and the diffusive and turbulent fluxes of latent and sensible heat fluxes from the land and vegetation surfaces. The timestep is 60 min to allow for calculation of the diurnal cycle of radiation.

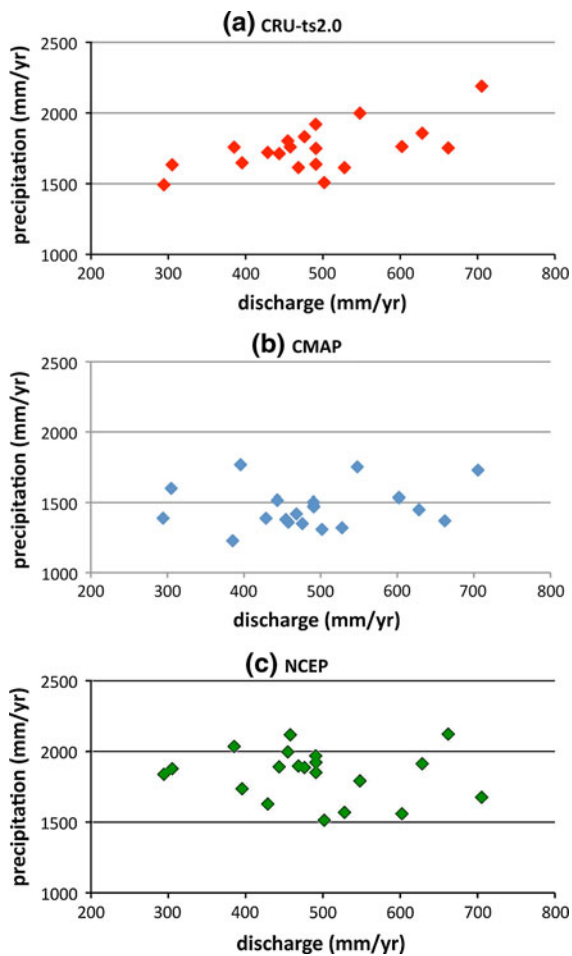


Fig. 3 Scatter diagrams of annual mean precipitation averaged for the Aruanã watershed versus observed discharge at the Aruanã gauge for the period 1980–1998 for **a** CRU-ts2.0, **b** CMAP, and **c** NCEP precipitation products. The sample size is 19 for each series

The soil column has six layers with a total depth of 8 m. Volumetric water content is simulated for each layer as a function of infiltration from the soil surface, vertical water movement, plant water use, and drainage from the bottom of the soil column. The soil water infiltration rate is calculated dynamically using a Green-Ampt formulation (Green and Ampt 1911) of the soil wetting front and its non-linear impact on maximum infiltration rates. The soil moisture simulation is based on Richards' flow equation and its change in time and space is a function root-water uptake and of soil physical properties, such as hydraulic conductivity, soil water retention curve, and drainage of water from the soil

column. Plant transpiration, which is the external driver of root water uptake, is governed by stomatal physiology. In IBIS, as in many models, transpiration is coupled to photosynthesis through the Ball-Berry formulation (Ball et al. 1986). Within the soil column the root-water uptake rate is controlled by soil physical properties (e.g. texture), the root distribution, and soil moisture profile (Kucharik et al. 2000; Li et al. 2005).

Surface runoff is simulated at each timestep as the water in excess of the precipitation landing on the surface and the soil infiltration. Sub-surface runoff is the water that drains from the bottom of the soil column and is therefore a dynamic function of the hydraulic conductivity and the plant water use. Horizontal runoff transport between grid cells is subsequently simulated by the THMB hydrological routing model and is described below.

THMB is a distributed grid hydrologic transport model that simultaneously calculates river discharge, lake area, and floodplain inundation (Coe et al. 2007). THMB uses prescribed river paths and river and floodplain morphology linked to a set of linear reservoir equations to calculate in-channel river volume, stage and discharge, and the out-of-channel floodplain volume, stage, and inundated area at a 1-h timestep and 5-min horizontal resolution (about 8 km × 8 km at the equator). At each timestep the change in the stream water volume in any grid cell in THMB is the sum of the surface runoff and sub-surface drainage from the fraction of the cell that is dry land, the precipitation and evaporation over the fraction of the cell that is covered with water, and the fluxes of water from the upstream grid cells minus the flux to the downstream cell. The flux to the downstream cell (discharge) is a function of the volume of water in the river reservoir, and is calculated using a Chezy formula (Dunne and Leopold 1978) that accounts for the effects of the energy slope of the water surface and frictional forces within the channel. Floodplain inundation occurs when the water level in the river exceeds the bankfull height. The flooded area is calculated as a function of the flux of water from the stream channel to the floodplain, the vertical water balance, the energy slope of the water, and the geomorphic characteristics of the river and floodplain. Mass in the river and floodplain reservoirs is explicitly conserved.

Together these models have been extensively calibrated, validated, and applied to the Amazon

basin (Botta and Foley 2002; Botta et al. 2002; Coe et al. 2002, 2007, 2009; Foley et al. 2002).

Numerical experiment design

Mean monthly surface and sub-surface runoff were generated by IBIS for input to THMB for the period January 1915 to December 2000 using the CRU-ts2 $0.5 \times 0.5^\circ$ horizontal resolution observed mean monthly climate variables of precipitation, temperature, humidity, wind speed, and cloudiness as climate forcing (Mitchell et al. 2004). IBIS was run at $0.5^\circ \times 0.5^\circ$ horizontal resolution with a time step of 1-h for basin. A stochastic weather generator within IBIS was used to derive daily and hourly climate values from the monthly climate data (Kucharik et al. 2000). The IBIS output from 1915–1960 was considered a spin-up period to assure that simulated soil moisture was in equilibrium with the climate and was not used.

The experimental design used in this study was similar to the design used by (Coe et al. 2009). First, two IBIS simulations were run with identical climate forcing and different vegetation cover: (1) IBIS-POT in which the vegetation was represented by the potential vegetation, predominantly savannah, that would be present without human intervention from Ramankutty and Foley (1998); and (2) IBIS-GRASS in which the entire basin was covered by C_4 grass. The resulting surface and sub-surface runoff represented idealized conditions in which no human disturbance had occurred (IBIS-POT) or large human land cover change had occurred (IBIS-GRASS).

Secondly, the IBIS-POT and IBIS-GRASS surface and sub-surface runoff data were linearly interpolated from the 0.5° resolution of IBIS to the 5-min resolution of THMB. Then the files were linearly mixed to create two new 5-min resolution datasets of surface and sub-surface runoff for the period 1970–2000 consistent with the heterogeneous land cover conditions in the 1970s and in the 1990s.

To create these 1970s and 1990s runoff scenarios, 5-min resolution maps of the fractional area of agriculture (disturbed) and native vegetation (undisturbed) in the 1970s and 1990s were used. The total surface or sub-surface runoff in each mixed 5-min grid cell was determined as the sum of IBIS-POT and IBIS-GRASS values over the undisturbed and disturbed fractions of that particular grid cell for the

1970s and 1990s maps (e.g. Fig. 1). For example, if in a particular 5-min grid cell there was no disturbance in the 1970s, then the surface and sub-surface runoff for the mixed file came entirely from the IBIS-POT simulation. In cases where the land cover was part disturbed and part undisturbed, the runoff input for a 5-min grid cell was a mix of both IBIS-POT and IBIS-GRASS based on the fraction of each land cover type present in the cell. Linear averaging of simulated results to create individual scenarios was appropriate because it closely approximated the linear averaging of the land cover types that occurred within each grid cell of IBIS.

The 1990s vegetation distribution used for generating the runoff files was taken from a 5-min resolution fractional agricultural area dataset for the mid-1990s created by (Cardille and Foley 2003). The Cardille and Foley dataset is a representation of the density of native vegetation, cropland, native pasture, and planted pasture at 5-min resolution. It was created by merging municipio-level agricultural census data with the 1-km resolution AVHRR-based University of Maryland land-cover classification product. A spatially explicit estimate of land use distribution was created for the 1970s in this study by dividing the Cardille and Foley estimate of agricultural fraction in each grid cell in the basin by two. This estimate reduced the total disturbed area to about 28%, which was consistent with estimates derived from census data for the region (Costa et al. 2003; Franco 2003; Klink and Machado 2005; Latrubesse et al. 2009). This simple method was chosen because it maintained consistency between the 1990s and 1970s data sets; the total disturbed area in both maps were based on census data for their respective period and the spatial distribution was rooted in satellite observations for the 1990s.

Finally, two simulations were run with THMB forced with the 1970s and 1990s surface and sub-surface runoff scenarios, referred to as RUN70 and RUN90, respectively. THMB was run at a 1-h timestep for the period 1960–2000. The years 1960–1969 were considered model spin-up and discarded. The remaining months from 1970–2000 were a representation of the river discharge throughout the Aruanã watershed as a function of the climate of that period and land cover distribution of the 1970s and 1990s. Any differences between RUN70 and RUN90 for the same time period were a result of the effect of land cover

differences on the runoff alone, since the climate that was used to create the runoff input files were identical in the two simulations.

Results

Observational data

Decadal mean observed discharge, for the Aruanã sub-basin, increased by 25% between the two decades, from a mean of 988 m³/s in the decade 1970–1979 to 1231 m³/s for 1990–1999 (Table 2). A *z*-test indicated that the difference in discharge between the 237 months in the decadal means was significant at the 0.0002 level. Decadal mean precipitation averaged over the same periods and region increased by 2.5% (from 4437 m³/s to 4546 m³/s) and the difference was not significant at the 0.05 level. The magnitude of the discharge change was 243 m³/s (or 93 mm/yr), which was more than twice the 109 m³/s (or 40 mm/yr) precipitation change. As a result, the decadal mean ratio of runoff to precipitation increased from 0.223 in the 1970s to 0.271 in the 1990s. A Student's *t*-test of the 20 years of data in the decadal means indicated that the difference of 0.048 in the ratio of runoff to precipitation was significant at the 0.0253 level (not shown).

The magnitude of the mean monthly discharge change was greatest during the middle of the wet season (January–March) but extended into August near the end of the dry season (Fig. 4). The discharge change was near zero for the beginning of the wet season (Sept.–Dec.). Observations of small watersheds show that peak flow is often earlier in deforested watersheds due to decreased soil water infiltration and greater surface runoff (Bruijnzeel 1991). In this study, there was no observed change in the timing of the peak discharge, which occurs in March in both decades (Fig. 4). The lack of a change in the time of peak flow suggested that no large change in soil infiltration rates or the ratio of surface to sub-surface runoff occurred between the decades.

The long-term mean water budget can be expressed as:

$$P - R = ET + \Delta S$$

where *P* is mean precipitation, *R* is total runoff (discharge), *ET* is the evapotranspiration, and ΔS is

Table 2 Climate statistics for the Aruanã watershed for the 1970s and 1990s

Aruanã		1970s	1990s	% change
Ag area		28%	56%	
Discharge m ³ /s	OBS	988	1231	25%
	RUN70	804	877	9%
	RUN90		1025	27%
%RE	RUN70	−19	−29	
	RUN90		−17	
<i>r</i>	RUN70	0.9308	0.8742	
	RUN90		0.9229	
P m ³ /s	OBS	4437	4546	2.5%
ET m ³ /s	OBS	3449	3315	−4%
	RUN70	3633	3669	0%
	RUN90		3521	−3%
R/P	OBS	0.223	0.271	22%
	RUN70	0.181	0.193	7%
	RUN90		0.225	24%
<i>z</i> -test	OBS-discharge		0.0002	
	OBS-precipitation		0.3651	
	RUN70		0.1156	
	RUN90		0.0019	

Ag area is the fraction of the 82,632 km² basin in agriculture. Decadal mean annual discharge (m³/s) and percent change for the 1970s and 1990s for: (1) observed at Aruanã (OBS); (2) simulated in RUN70 with the climate of the 1970s and 1990s but with fixed 1970s vegetation; and (3) simulated in RUN90 with 1990s vegetation and climate. Percent relative error (%RE) of the simulated decadal mean discharge of RUN70 and RUN90 compared to the observed discharge. Pearson product moment correlation coefficient (*r*) between the 12 decadal mean monthly values of simulated discharge and the 12 monthly observed values. Decadal mean annual observed precipitation (*P*) in m³/s for each decade and percent change. Evapotranspiration (*ET*) in m³/s for each decade calculated as the difference between precipitation and discharge for the observations (OBS), RUN70 and RUN90. The ratio of discharge to precipitation (*R/P*) for observations (OBS), RUN70, and RUN90. *Z*-test of the difference in the 240 months of data in the 1990s and 1970s monthly means for observed discharge and precipitation and for RUN70 and RUN90 simulated discharge. In the case of RUN90 the *z*-test is performed on the 120 months in the RUN90 simulated 1990s to the 120 months in the RUN70 simulated 1970s. Similarly, all RUN90 differences are calculated as the difference between RUN90 in the 1990s and RUN70 in the 1970s (i.e. RUN90 value in 1990s column is compared to the RUN70 value in the 1970s column)

the net change in groundwater storage. Generally, ΔS is considered to be equal to 0 for long-term means and *ET* can be calculated as:

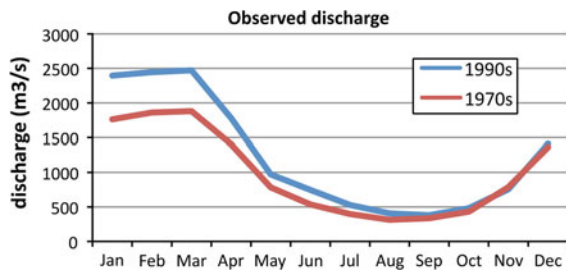


Fig. 4 Decadal mean monthly observed discharge in m^3/s at Aruanã for the 1970s and 1990s

$$P - R = ET$$

Using this equation, and the values of P and R (discharge) from Table 2, decadal mean ET must have decreased from 3449 in the 1970s to 3315 m^3/s in the 1990s, which is equivalent to a 4% decrease (Table 2).

Although the precipitation increase between the 1990s and 1970s was not statistically significant it decreased the confidence that the observed increase in the water yield and discharge were largely independent of the precipitation change. In order to address this, 5-year sub-sets of the 1970s and 1990s data were compared to reduce the precipitation difference between the decades. Water years 1972, 73, 74, 77, 78 were averaged and compared to water years 1993, 94, 96, 97, and 98 (not shown). These years were chosen because they represented the middle-range of the available data, all years had an annual mean precipitation rate between 1700 and 1850 mm/yr . For this 5-year mean comparison the mean rainfall rate was 1% lower in the 1990s than in the 1970s and the difference was not significant at the 0.05 level (not shown). The mean discharge rate for these years was 16% higher in the 1990s than the 1970s. A z -test of the 120 months in the two 5-year averages indicated that the discharge of the 1990s differed from the 1970s at the 0.05 significance level. This additional analysis suggested that there was a significant difference in the surface water balance of the 1970s and the 1990s that could not be explained by precipitation changes alone.

Model results

In RUN70, the discharge for the Aruanã watershed was simulated with the transient mean monthly climate of the 1970–2000 period and land cover held

constant to the 1970s estimate ($\sim 28\%$ deforested). The results of RUN70 provided a measure of the influence of climate variability alone on the discharge difference between the 1990s and 1970s.

The RUN70 mean discharge for the 1970s decade was 804 m^3/s compared to the observed discharge of 988 m^3/s (Table 2). The Pearson correlation coefficient (r) between simulated and observed discharge for the 12 monthly mean values was 0.9308 (Table 2, Fig. 5a). The percent relative error (RE) statistical index of the RUN70 mean monthly discharge for the 1970s decade compared to the observed was -19% , which indicated a systematic dry bias in the simulated discharge. The simulated runoff ratio was 0.0181 compared to 0.223 for the observations. The modeled dry bias may have been a result of several unknown factors such as: a dry bias in the precipitation data, biases in the calculation of the water and energy balance of IBIS, and poor representation of the land surface and vegetation characteristics such as, rooting depth, root water extraction, soil properties etc.

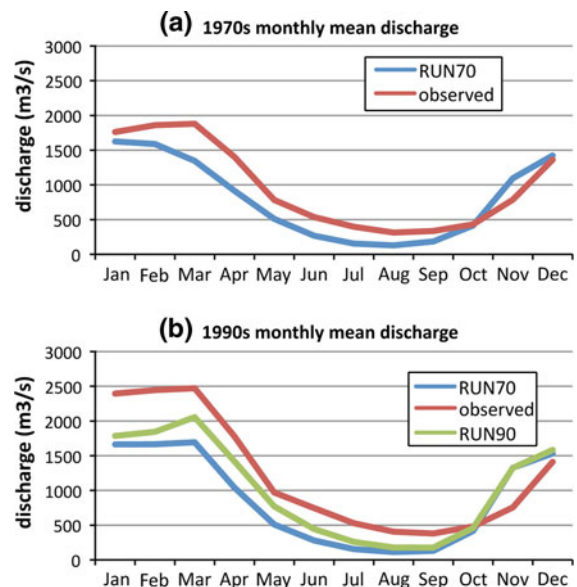


Fig. 5 Decadal mean monthly discharge in m^3/s at the Aruanã station for the observations, RUN70 simulation, and RUN90 simulation at Aruanã. **a** 1970s decadal mean and **b** 1990s decadal mean. RUN70 has the transient climate of the period 1970–2000 with land cover fixed to the 1970s mean distribution of about 28% deforested. RUN90 has the transient climate of the period with the land cover fixed to the 1990s mean distribution of about 56% deforested. Differences between RUN70 and RUN90 in the 1990s (**b**) are attributable solely to the land cover differences

However, the bias did not necessarily preclude an analysis of the relative change between decades since the climate and the model were identical in all simulations and the relative error should have been similar in all simulations.

The 1990s simulated decadal mean discharge from RUN70 showed much poorer agreement with the observations than the 1970s decadal mean. The %RE increased to -29% in the 1990s and the coefficient of correlation decreased to 0.8742 (Table 2, Fig. 5a, b). In RUN70 the simulated mean discharge of the 1990s (Table 2, $877 \text{ m}^3/\text{s}$) was only 9% greater than the simulated 1970s discharge ($804 \text{ m}^3/\text{s}$). The difference between the 1990s and 1970s discharge simulated in RUN70 was not significant at the 0.05 level and was much less than the 25% increase in the observed discharge for this period (Table 2, Figs. 4, 5). The simulated RUN70 runoff ratio increased only slightly between the 1970s and 1990s and the difference was not significant at the 0.05 level (not shown). Furthermore, the inferred mean ET for the Aruanã watershed (precipitation minus discharge) increased between the two decades by 1% (from 3633 to $3669 \text{ m}^3/\text{s}$) as opposed to the 4% decrease in the observed ET (Table 2). Land cover was held constant in RUN70 therefore the modest increase in simulated discharge and ET between the two decades in RUN70 was due exclusively to the variability of the climate data that was used as input to IBIS. The RUN70 results showed that using climate variability alone, a simulated discharge increase comparable to the 25% increase in the observed discharge could not be achieved.

In RUN90 land cover changes and climate variability were included in the 1990s simulation and the agreement of the simulated 1990s discharge with the observed discharge was improved. The coefficient of correlation between the 24 monthly mean simulated and observed values for the 1990s was 0.9229 and the %RE of the simulated discharge was -17% , compared to -29% for the RUN70 simulated 1990s discharge. This agreement with the observations was comparable to the agreement between simulated and observed discharge in RUN70 with 1970s climate and land cover described in the previous paragraph (Table 2). Therefore, the RUN90 results showed that the simulated discharge was in good agreement with the observations of the 1990s only when land cover and climate variability were included in the simulation.

Comparison of the simulated 1990s and 1970s results when both climate and land cover were consistent with the respective decades (i.e. comparison of RUN90 in 1990s to RUN70 in the 1970s) showed that the observed discharge difference between the decades is well reproduced by the models when both land cover changes and climate variability were included (Table 2). The 1990s RUN90 discharge was 27% greater than the 1970s RUN70 discharge (Table 2, $1025 \text{ m}^3/\text{s}$ in 1990s minus $804 \text{ m}^3/\text{s}$ in the 1970s) and the difference was significant at the 0.0019 level. The increase in simulated discharge was comparable to the 25% increase in the observed discharge for this period and larger than the 9% increase simulated for the 1990s without land cover change (Table 2, Fig. 5). The inferred ET decrease was 3%, which was comparable to the 4% decrease in the observed data and the runoff ratio increased by 0.044 (significant at the 0.0063 level), similar to the 0.048 change in the observed runoff ratio. Therefore, the simulated change in the surface water balance between the decades agreed with the observed change only when both climate variability and land cover change were included in the simulation.

An analysis of the individual components of the simulated discharge showed that of the $221 \text{ m}^3/\text{s}$ (27%) increase from 1970s to the 1990s, about 33% of the increase was from climate variation (the 9% increase between the 1970s and 1990s decades in RUN70) and about 67% was a result of land cover change (18% additional change in RUN90, Table 2).

Discussion and conclusions

Agricultural expansion, which began in the 1960s, resulted in deforestation of about 25% of the $82,632 \text{ km}^2$ study region of the Araguaia River upstream of the Aruanã gauge station by the middle 1970s and 55% by the middle 1990s. Over the same period, significant changes in the surface water balance were observed. The decadal mean discharge rate increased by 25% in the 1990s compared to the 1970s, while the precipitation rate was only 2.5% greater in the 1990s. The magnitude of the discharge change was more than twice the magnitude of the precipitation change and as a result, the decadal mean runoff ratio increased from about 22% of the precipitation in the 1970s to about 27% in the 1990s.

A comparison of a sub-set of the data showed that the change in the runoff ratio and discharge during this period were largely independent of a precipitation change. When only 5 years from each decade were used for comparison the rainfall rate was 1% less in the 1990s than in the 1970s, but the discharge rate was nearly 16% greater. Therefore, the observations indicated that a significant change in the surface water budget occurred between the 1970s and 1990s that was most likely not associated with precipitation variation.

A classical water balance calculation requires that the precipitation and runoff change must be balanced by an equal change in the sum of evapotranspiration and net groundwater storage. The change in the observed precipitation and discharge implied that decadal mean ET must have decreased by 4% in the 1990s compared to the 1970s, if it is assumed that no net change in groundwater storage occurred. The ET decrease could have been from climate variations, such as some combination of differences in precipitation, net radiation, and temperature, from a reduction in the vegetation density and total evaporative demand, or some combination of both. In a relatively dry and strongly seasonal climate like the Aruanã basin, ET tends to increase with increasing precipitation since the region is water limited rather than energy limited (Costa et al. 2003). Additionally, observations at regional and small scales in the tropics showed that deforestation and forest degradation were generally accompanied with a decrease in ET (Bruijnzeel 1990, 1991; Costa et al. 2003; Giambelluca et al. 2009; Hayhoe et al. 2010). Therefore, a plausible cause of at least part of the inferred ET decrease was the observed shift from the native mixed forest and grassland Cerrado to pasture and cropland landscape.

Latrubesse et al. (2009) showed that large morphological changes also occurred in the Araguaia River since the 1970s and attributed those changes to deforestation. They calculated that the bed load sediment transport at Aruanã increased ~31%, from ~6.75 Mt/yr in the 1970s to ~8.9 Mt/yr in the 1990s and an average of ~95 Mt of sandy and fine sediments averaging 6.7 m thickness were stored during this period, principally in the main channel valley. The river metamorphosed in some extensions, losing part of the anabranching pattern and developed a more braided pattern with an increase in the number

of sandy middle channel bars in place of more stable vegetated islands.

Taken together the observed discharge, morphologic, and sediment flux changes are consistent with hydromorphic changes that accompany deforestation and conversion to agriculture: the mobilization of sediments from the land surface, decreased evapotranspiration, increased water yield and surface runoff, and increased river discharge (Bosch and Hewlett 1982; Bruijnzeel 1990; Bruijnzeel 1991; Knox 1972; Knox 2006).

Numerical model simulations can help clarify the drivers of environmental change because they integrate climate and land cover changes to calculate a linked water and energy balance and because they can be manipulated in a controlled manner. We presented the results of simulations with the IBIS and THMB land surface models of the water budget of the Aruanã watershed in the 1970s and 1990s with and without land cover change. The models reproduced a discharge change of the same magnitude as the observed change, only when both precipitation and land cover changes were included in the simulations. The precipitation change by itself resulted in a 9% increase in simulated discharge in the 1990s compared to the 1970s. Precipitation and deforestation together resulted in a 27% increase in the simulated discharge, which was comparable to the observed 25% increase.

As with all modeling studies the results presented in this study are strongly dependent on the model representation of the physical environment and on the experimental design and their uncertainty are not easily quantified. IBIS has been calibrated and validated for the Amazon with historical and future climate and its sensitivity to land cover differences has been validated in previous studies (Coe et al. 2007, 2009; Li et al. 2007). The sensitivity of simulated ET to land cover change is a function of model specific parameters such as plant root structure, soil properties, and above ground biomass, which are not well known. Furthermore, the representation of deforestation and conversion to agriculture in this study is simplistic; all deforested areas are considered to be 100% C₄ grass. Secondary regrowth and mixed landscapes such as natural pastures in which some trees remain on the landscape are not simulated. Therefore, the results must be considered an analysis of the scale of change that may occur with disturbance rather than an exact prediction of the change.

Despite the limitations of numerical models several important points were suggested by the model results. The simulation without land cover change suggested that about 1/3 of the observed discharge increase in the 1990s can be attributed to the observed increase in precipitation. The simulation with land cover change compared to that without land cover change in the 1990s suggested that the remaining 2/3 of the observed discharge increase was most likely the result of some other factor such as a net decrease in evapotranspiration that occurred when native vegetation was replaced with more shallow rooted, less water-demanding pastures and crops.

The deforestation recorded in the census data in this segment of the Araguaia River is comparable to what has occurred throughout much of the 2,000,000 km² Cerrado region and what is beginning to occur in the tropical evergreen ecosystem of the southern Amazon as regional and global food and energy demands drive pasture and farmland expansion (Nepstad et al. 2008; Sano et al. 2009). The observed and simulated results in this and other recent studies (Coe et al. 2009; Costa et al. 2003), suggest that similar, but mostly undocumented, hydrological and morphological changes may already be occurring in many other large river systems in the Cerrado. The results also suggest that continued local and federal efforts to expand protected regions and strengthen compliance with existing laws, which limit deforestation on private parcels and protect riparian zones, could avoid or reverse detrimental changes in the hydrological and morphological state of many of the major rivers of the Cerrado and southern Amazon regions.

Acknowledgments We gratefully acknowledge the contributions of Paul Lefebvre in developing figures, Dr. Eric A. Davidson and Wendy Kinglerlee's helpful comments, and Dr. Hewlley Acioli's help with precipitation data. We also thank two anonymous reviewers for comments that greatly improved the manuscript. Funding was provided by the United States National Aeronautics and Space Administration, Land Cover and Land Use Change and LBA-ECO programs, CNPq-Brazil, CYTED, and VITAE Foundation.

References

- Achard F, Eva HD, Stibig H-J, Mayaux P, Gallego J, Richards T, Malingreau J-P (2002) Determination of deforestation rates of the world's humid tropical forests. *Science* 297:999–1002
- Ball JT, Woodrow IE, Berry JA (1986) A model predicting stomatal conductance and its contribution to the control of photosynthesis under different light conditions. In: Biggins J (ed) *Progress in photosynthetic research*. M. Nijhoff Publishers, Dordrecht, pp 221–224
- Bonan GB, DeFries RS, Coe MT, Ojima DS (2004) Land use and climate. In: Gutman G (ed) *Land change science*. Kluwer Academic Publishers, Amsterdam, pp 301–314
- Bosch JM, Hewlett JD (1982) A review of catchment experiments to determine the effect of vegetation changes on water yield and evapotranspiration. *J Hydrol* 55:3–23
- Botta A, Foley JA (2002) Effects of climate variability and disturbances on the Amazonian terrestrial ecosystems dynamics. *Global Biogeochem Cycles* 16:1–11
- Botta A, Ramankutty N, Foley JA (2002) Long-term variations of climate and carbon fluxes over the Amazon basin. *Geophys Res Lett* 29:1–4
- Bruijnzeel LA (1990) Hydrology of moist tropical forests and effects of conversion: a state of knowledge review. UNESCO, Paris
- Bruijnzeel LA (1991) Hydrological impacts of tropical forest conversion. *Nature Resour* 27:36–46
- Canadell J, Jackson RB, Ehleringer JR, Mooney HA, Sala OE, Schulze ED (1996) Maximum rooting depth of vegetation types at the global scale. *Oecologia* 108:583–595
- Cardille JA, Foley JA (2003) Agricultural land-use change in Brazilian Amazonia between 1980 and 1995: evidence from integrated satellite and census data. *Remote Sens Environ* 87:551–562
- Coe MT, Costa MH, Botta A, Birkett C (2002) Long-term simulations of discharge and floods in the Amazon basin. *J Geophys Res* 107:1–17
- Coe MT, Costa MH, Howard EA (2007) Simulating the surface waters of the Amazon River Basin: impacts of new river geomorphic and dynamic flow parameterizations. *Hydrol Process* 21:2542–2553
- Coe MT, Costa MH, Soares-Filho BS (2009) The Influence of historical and potential future deforestation on the stream flow of the Amazon River—land surface processes and atmospheric feedbacks. *J Hydrol* 369:165–174
- Costa M, Foley J (1997) Water balance of the Amazon Basin: dependence on vegetation cover and canopy conductance. *J Geophys Res* 102:23973–23989
- Costa MH, Botta A, Cardille JA (2003) Effects of large-scale changes in land cover on the discharge of the Tocantins River, Southeastern Amazonia. *J Hydrol* 283:206–217
- Dunne T, Leopold LB (1978) *Water in environmental planning*. W.H. Freeman and Company, New York
- Eagleson PS (1978) Climate, soil, and vegetation 1. Introduction to water balance dynamics. *Water Resour Res* 14:705–712
- Fearnside PM (2005) Deforestation in Brazilian Amazonia: history, rates and consequences. *Conserv Biol* 19:680–688
- Ferreira LG, Asner GP, Knapp DE, Davidson EA, Coe MT, Bustamante MMC, Oliveira EL (in press) Equivalent water thickness in savanna ecosystems: MODIS estimates based on ground and EO-1 Hyperion data. *Int J Remote Sens*
- Fetter CW (2001) *Applied hydrogeology*. Prentice Hall, New Jersey
- Foley JA, Botta A, Coe MT, Costa MH (2002) El Niño-Southern oscillation and the climate, ecosystems and rivers of Amazonia. *Global Biogeochem Cycles* 16:1–17

- Franco SM (2003) O grande vale do Araguaia: transformações da bacia do Araguaia e Goiás. Instituto de Estudos Sócio Ambientais, Universidade Federal de Goiás, Goiânia, p 382
- Garcia-Montiel DC, Coe MT, Cruz MP, Ferreira JN, da Silva EM, Davidson EA (2008) Estimating seasonal changes in volumetric soil water content at landscape scales in a Savanna ecosystem using two-dimensional resistivity profiling. *Earth Interact* 12:1–25
- Gardner WR (1983) Soil properties and efficient water use: an overview. In: Taylor HM, Jordan WR, Sinclair TR (eds) Limitations to efficient water use in crop production. American Society of Agronomy, Madison, WI, pp 45–46
- Giambelluca TW, Scholz FG, Bucci SJ, Meinzer FC, Goldstein G, Hoffmann WA, Franco AC, Buchert MP (2009) Evapotranspiration and energy balance of Brazilian savannas with contrasting tree density. *Agric For Meteorol* 149:1365–1376
- Green WH, Ampt GA (1911) Studies on soil physics, 1. The flow of air and water through soils. *J Agric Sci* 4:1–24
- Hayhoe S, Neill C, McHorney R, Porder S, Lefebvre P (2010) Amazon forest conversion to soy agriculture increases stream discharge but not stormflow. *Glob Change Biol*. doi:10.1111/j.1365-2486.2011.02392.x
- Kaimowitz D, Mertens B, Wunder S, Pacheco P (2004) Hamburger connection fuels Amazon destruction. Center for International Forest Research, Bangor, Indonesia
- Kalnay E, Kanamitsu M, Kistler R (1996) The NCEP/NCAR 40-year reanalysis project. *Bull Am Meteorol Soc* 77:437–471
- Kistler R (2001) The NCEP-NCAR 50-year reanalysis: monthly means CD-ROM and documentation. *Bull Am Meteorol Assoc* 82:247–267
- Klink CA, Machado RB (2005) Conservation of the Brazilian Cerrado. *Conserv Biol* 19:707–713
- Knox JC (1972) Alluviation in Southwestern Wisconsin. *Ann Assoc Am Geogr* 62:401–410
- Knox JC (2006) Floodplain sedimentation in the Upper Mississippi Valley: natural versus human accelerated. *Geomorphology* 79:286–310
- Kucharik CJ, Foley JA, Delire C, Fisher VA, Coe MT, Lenters JD, Young-Molling C, Ramankutty N, Norman JM, Gower ST (2000) Testing the performance of a dynamic global ecosystem model: water balance, carbon balance, and vegetation structure. *Global Biogeochem Cycles* 14:795–825
- Latrubesse EM (2008) Patterns of anabranching channels: the ultimate end member adjustment of mega rivers. *Geomorphology* 101:130–145
- Latrubesse EM, Amsler M, Morais M, Aquino S (2009) The geomorphological response of a large pristine alluvial river to tremendous deforestation in the South American Tropics: the case of the Araguaia River. *J Geomorphol* 113:239–252
- Li KY, Coe MT, Ramankutty N (2005) Investigation of hydrological variability in West Africa using land surface models. *J Clim* 18:3173–3188
- Li KY, Coe MT, Ramankutty N, De Jong R (2007) Modeling the hydrological impact of land-use change in West Africa. *J Hydrol* 337:258–268
- Meinzer FC, Andrade JL, Goldstein G, Holbrook NM, Cavelier J, Wright SJ (1999a) Partitioning of soil water among canopy trees in a seasonally dry tropical forest. *Oecologia* 121:293–301
- Meinzer FC, Goldstein G, Franco AC, Bustamante M, Iglar E, Jackson P, Caldas L, Rundel PW (1999b) Atmospheric and hydraulic limitations on transpiration in Brazilian cerrado woody species. *Funct Ecol* 13:273–282
- Meinzer FC, Brooks JR, Bucci SJ, Goldstein G, Scholz FG, Warren JM (2004) Converging patterns of uptake and hydraulic redistribution of soil water in contrasting woody vegetation types. *Tree Physiol* 24:919–928
- Mitchell TD, Carter T, Jones P, Hulme M, New M (2004) A comprehensive set of high-resolution grids of monthly climate for Europe and the globe: the observed record (1901–2000) and 16 scenarios (2001–2100). Tyndall Centre working paper (p 25). Tyndall Center for Climate Change Research.
- Moreira MZ, Scholz FG, Bucci SJ, Sternberg LS, Goldstein G, Meinzer FC, Franco AC (2003) Hydraulic lift in a neotropical savanna. *Funct Ecol* 17:573–581
- Myers N, Mittermeier RA, Mittermeier CG, Fonseca GAB, Kent J (2000) Biodiversity hotspots for conservation priorities. *Nature* 403:853–858
- Nepstad DC, Stickler CM, Soares Filho BS, Merry F (2008) Interactions among Amazon land use, forests and climate: prospects for a near-term forest tipping point. *Philos Trans R Soc* 363:1737–1746
- Oliveira RS, Bezerra L, Davidson EA, Pinto F, Klink CA, Nepstad DC, Moreira A (2005) Deep root function in the soil water dynamics in cerrado savannas of central Brazil. *Funct Ecol* 19:574–581
- Ramankutty N, Foley JA (1998) Characterizing patterns of global land use: an analysis of global croplands data. *Global Biogeochem Cycles* 12:667–685
- Raymond PA, Oh NH, Turner RE, Broussard W (2008) Anthropogenically enhanced fluxes of water and carbon from the Mississippi River. *Nature* 451:449–452
- Sano EE, Rosa R, B JL, Ferreira LG (2008) Semidetailed land use mapping in the Cerrado. *Pesquisa Agropecuária Brasileira* 43:153–156
- Sano EE, Rosa R, Brito JLS, Ferreira LG (2009) Land cover mapping of the tropical savanna region in Brazil. *Environ Monit Assess* 166:113–124
- Santos AJB, Quesada CA, da Silva GT, Maia JF, Miranda HS, Miranda AC, Lloyd JL (2004) High rates of net ecosystem carbon assimilation by Brachiaria pasture in the Brazilian Cerrado. *Glob Change Biol* 10:877–885
- Scholz FG, Bucci SJ, Goldstein G, Meinzer FC, Franco AC (2002) Hydraulic redistribution of soil water by neotropical savanna trees. *Tree Physiol* 22:603–612
- Scholz FG, Bucci SJ, Goldstein G, Moreira MZ, Meinzer FC, Domec J-C, Vega RV, Franco AC, Miralles-Wilhelm F (2008) Biophysical and life history determinants of hydraulic lift in Neotropical savanna trees. *Funct Ecol* 22:773–786
- Xie P, Arkin PA (1997) Global precipitation: a 17-year monthly analysis based on gauge observations, satellite estimates, and numerical model outputs. *Bull Am Meteorol Soc* 78:2539–2558